Acta Pharmaceutica Sinica B 2019;9(2):304–315

Chinese Pharmaceutical Association
Institute of Materia Medica, Chinese Academy of Medical Sciences

Acta Pharmaceutica Sinica B

www.elsevier.com/locate/apsb
www.sciencedirect.com

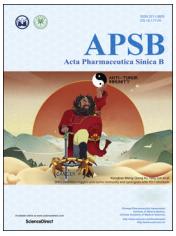

ORIGINAL ARTICLE

SHP2 inhibition triggers anti-tumor immunity and synergizes with PD-1 blockade

Mingxia Zhao[a,†], Wenjie Guo[a,†], Yuanyuan Wu[b,†], Chenxi Yang[a], Liang Zhong[c], Guoliang Deng[a], Yuyu Zhu[a], Wen Liu[a], Yanhong Gu[d], Yin Lu[b], Lingdong Kong[a], Xiangbao Meng[a,c,*], Qiang Xu[a,*], Yang Sun[a,*]

[a]*State Key Laboratory of Pharmaceutical Biotechnology, Deparment of Biotechnology and Pharmaceutical Sciences, School of Life Sciences, Nanjing University, Nanjing 210023, China*
[b]*Jiangsu Key Laboratory for Pharmacology and Safety Evaluation of Chinese Materia Medica, School of Pharmacy, Nanjing University of Chinese Medicine, Nanjing 210023, China*
[c]*State Key Laboratory of Natural and Biomimetic Drugs, Department of Chemical Biology, School of Pharmaceutical Sciences, Peking University, Beijing 100191, China*
[d]*Department of Oncology, the First Affiliated Hospital with Nanjing Medical University, Nanjing 210029, China*

Received 16 July 2018; received in revised form 18 August 2018; accepted 30 August 2018

KEY WORDS

Cancer immunotherapy;
SHP2;
SHP099;
PD-1;
Colon cancer

Abstract Tyrosine phosphatase SHP2 is a promising drug target in cancer immunotherapy due to its bidirectional role in both tumor growth promotion and T-cell inactivation. Its allosteric inhibitor SHP099 is known to inhibit cancer cell growth both *in vitro* and *in vivo*. However, whether SHP099-mediated SHP2 inhibition retards tumor growth *in vivo via* anti-tumor immunity remains elusive. To address this, a CT-26 colon cancer xenograft model was established in mice since this cell line is insensitive to SHP099. Consequently, SHP099 minimally affected CT-26 tumor growth in immuno-deficient nude mice, but significantly decreased the tumor burden in CT-26 tumor-bearing mice with intact immune system. SHP099 augmented anti-tumor immunity, as shown by the elevated proportion of $CD8^{+}IFN\text{-}\gamma^{+}$ T cells and the upregulation of cytotoxic T-cell related genes including *Granzyme B andPerforin*, which decreased the tumor load. In addition, tumor growth in mice with SHP2-deficient T-cells was markedly slowed down because of enhanced anti-tumor responses. Finally, the combination of SHP099 and anti-PD-1 antibody showed a higher therapeutic efficacy than either monotherapy in controlling tumor growth

*Corresponding authors. Tel./fax +86 25 89687620.
E-mail addresses: xbmeng@bjmu.edu.cn (Xiangbao Meng), molpharm@163.com (Qiang Xu), yangsun@nju.edu.cn (Yang Sun).
†These authors made equal contributions to this work.

Peer review under responsibility of Institute of Materia Medica, Chinese Academy of Medical Sciences and Chinese Pharmaceutical Association.

https://doi.org/10.1016/j.apsb.2018.08.009

in two colon cancer xenograft models, indicating that these agents complement each other. Our study suggests that SHP2 inhibitor SHP099 is a promising candidate drug for cancer immunotherapy.

1. Introduction

T-cells are activated through a combination of antigen-specific signals from the T-cell receptor (TCR) and antigen-independent signals from the co-stimulatory receptors. In addition, several co-inhibitory receptors are also expressed on the T-cells which mediate inhibitory signals and balance T-cell activation[1]. These co-inhibitory receptors, also known as immune checkpoints, include the programmed cell death 1 (PD-1) and cytotoxic T-lymphocyte-associated protein 4 (CTLA-4), and play important roles in maintaining peripheral tolerance and immune homeostasis[2]. However, this same homeostasis mechanism is utilized by the tumors to escape immune surveillance[3]. Programmed death-ligand 1 (PD-L1), which is frequently expressed on tumor cells, inhibits naive and effector T-cell responses by binding to PD-1[4]. In recent years, cancer immunotherapy based on blocking PD-1/PD-L1 interaction has shown encouraging results. Immune checkpoint inhibitors like pembrolizumab, nivolumab and atezolizumab have been approved by U. S. Food and Drug Administration (FDA) for the second-line treatment of non-small cell lung cancer (NSCLC). In September 2017, the combination of chemotherapy and Keytruda®/pembrolizumab was approved as the first-line treatment for patients with metastatic non-squamous NSCLC[5]. In addition, other inhibitory receptors such as lymphocyte-activation gene 3 (LAG-3), T cell immunoglobulin (TIM-3), and V-domain Ig suppressor of T cell activation (VISTA) have recently emerged as new potential targets[6–8]. However, immune-checkpoint based cancer therapy still has several limitations such as inadequate response rate, and the lack of optimal biomarkers to predict response and toxicity.

SHP2 is a non-receptor ubiquitous protein tyrosine phosphatase encoded by the *PTPN11* gene in humans, with a relatively conserved structure and function[9]. It contains a protein tyrosine phosphatase catalytic domain (PTP domain), two SH2 domains and a C-terminal tail with two tyrosine phosphorylation sites and a proline-rich motif. SHP2 activity is auto-inhibited by the binding of N-SH2 domain with the PTP domain[10]. Upon stimulation by growth factors or cytokines, the N-SH2 domain binds to specific phospho-tyrosine residues to induce a conformational change, which exposes and catalytically activates the PTP domain[11], contributing to SHP2 activation and tumorigenesis[12–16]. As an oncogene, SHP2 regulates cancer cell survival and proliferation primarily by activating the RAS-ERK signaling pathway[17]. Recently, Chen et al.[16] found that cancer cell lines sensitive to SHP2 depletion were also sensitive to EGFR depletion, which validated reports that RTK-driven cancer cells depend on SHP2 for survival. Furthermore, recent studies have shown that SHP2 is required for the growth of mutant KRAS-driven cancers while wild-type KRAS-amplified gastroesophageal cancer can be controlled through combined SHP2 and MEK inhibition[18–20].

As a downstream target of several receptors, SHP2 is also involved in signaling in T-cells[21,22]. It is a downstream molecule in the PD-1 signaling pathway which not only suppresses T-cell activation but also causes T-cell anergy[23–25]. Our previous study showed that SHP2-deficiency in T-cells triggered an anti-tumor immune response against colitis-associated cancer in mice[26]. Therefore, targeting SHP2 may restore or even enhance T-cell functions. In the present study, we examined the effect of SHP099, a novel potent allosteric inhibitor of SHP2, on xenograft tumor models. We found that pharmacological inhibition of SHP2 decreased tumor burden by augmenting $CD8^+$ cytotoxic T-cell mediated anti-tumor immunity. In addition, conditional knockout of SHP2 in T-cells also inhibited tumor growth *in vivo* by the same mechanism. Finally, SHP2 inhibition synergized with PD-1 blockade in MC-38 and CT-26 tumor-bearing mice. Our results suggest that the SHP2 allosteric inhibitor SHP099 is a promising drug candidate for cancer immunotherapy.

2. Materials and methods

2.1. Mice

T lymphocyte-specific SHP2 knockout mice ($Ptpn11^{Cd4-/-}$) were generated by crossing $Ptpn11^{flox/flox}$ mice with *Cd4*-Cre transgenic mice. Female BALB/c or C57BL/6 mice (6–8 weeks old) were purchased from Model Animal Research Center of Nanjing University (Nanjing, China), and maintained in a specific-pathogen-free (SPF) facility with 12-h light/dark cycles, and had *ad libitum* access to food and water. The animals were treated humanely and all experimental procedures were carried out in accordance with the Guide for the Care and Use of Laboratory Animals, with the approval of the Animal Care and Use Committee of Nanjing University (Nanjing, China). All efforts were made to reduce the number of animals used and to minimize their suffering.

2.2. Cells

CT-26 cells were obtained from the Cell Bank of the Chinese Academy of Sciences. MC-38 cells were obtained from Cell Resource Center of the Institutes of Biomedical Sciences at Fudan University (Shanghai, China). Cells were maintained in the appropriate culture medium suggested by suppliers. The adult peripheral blood samples were obtained from five healthy donors at Nanjing Drum Tower Hospital (Nanjing, China) and the experimental protocols were performed according to the approved guidelines established by the Human Research Subjects Medical Ethics Committee of Nanjing University (Nanjing, China).

2.3. Chemicals, reagents and antibodies

SHP099 and SHP099 hydrochloride (purity > 99%) were synthesized by Prof. Xiangbao Meng (School of Pharmaceutical Sciences, Peking University, Beijing, China) with the detailed information in Supplementary data. Anti-PCNA antibody (sc-56) was purchased from Santa Cruz Biotechnology (Santa Cruz, CA, USA). GTVisin™ anti-mouse/anti-rabbit immunohistochemistry analysis kit was

purchased from Gene Company Ltd. (Shanghai, China). Purified anti-mouse PD-1 (clone RMP1–14) was purchased from BioXcell (West Lebanon, NH, USA). Anti-mouse CD3e monoclonal antibody (16-0031-82) and anti-mouse CD28 monoclonal antibody (16-0281-82) were purchased from eBioscience (San Diego, CA). Anti-human CD3 (16-0036-81) and anti-human CD28 (16-0289-81) were purchased from Thermo Fisher Scientific (Waltham, MA, USA). For flow cytometry analysis, anti-CD4 (7150784), anti-CD8 (7051685), anti-IFN-γ (7081524) and anti-TNF-α (7159734) antibodies were purchased from BD Pharmingen (San Diego, CA, USA). Anti-granzyme B (GZMB, B256443) and anti-perforin (PRF, B256234) were purchased from BioLegend (San Diego, CA, USA). For immunohistochemistry, anti-GZMB (46890) was purchased from Cell Signaling Technology (Beverly, MA, USA) and anti-IFN-γ (ab9657) was purchased from Abcam (Cambridge, UK). Mouse CD8a MicroBeads (130-117-044) was purchased from Miltenyi Biotec (Bergisch Gladbach, Germany). TUNEL Bright-Green Apoptosis Detection Kit (A112-02) was purchased from Vazyme (Nanjing, China). All other chemicals were purchased from Sigma–Aldrich (Shanghai, China).

2.4. *In vivo xenograft mouse model*

CT-26 cells and MC-38 cells were subcutaneously inoculated into BALB/c mice (1×10^6) and C57BL/6 mice (1×10^6), respectively. From day 3 post-inoculation, tumor dimensions were measured every day and the tumor size was calculated as $0.5 \times \text{length} \times \text{width}^2$. The mice were euthanized when tumor size was larger than 20 mm at the longest axis. Tumor-bearing mice with similar size were randomized into 5 groups that received PBS, 5-Fu, SHP099, anti-PD-1 antibody or SHP099 plus anti-PD-1 antibody, respectively. SHP099 hydrochloride was intraperitoneally injected at 5 mg/kg every day, and anti-PD-1 antibody was intraperitoneally injected at 5 mg/kg every 3 days.

2.5. *T-cell and tumor-infiltrating lymphocyte isolation*

Primary $CD8^+$ T-cells were isolated from the spleens of C57BL/6 mice using CD8 MicroBeads (Miltenyi) according to the manufacturer's instructions. The tumor-infiltrating lymphocytes were isolated using 40%–70% Percoll (Beyotime) gradient centrifugation after digesting the tissues with collagenase IV (Beyotime). To analyze the effector function of $CD8^+$ T-cells within that fraction, the cells were stimulated with 50 ng/mL phorbol 12-myristate 13-acetate (PMA) and 1 μmol/L ionomycin for 4 h in the presence of 5 μg/mL BFA, and then stained with FITC-anti-CD4, PerCP-Cy5.5-anti-CD8a and PE-anti-IFN-γ antibodies for flow cytometry assay.

2.6. *Quantitative reverse-transcriptase polymerase chain reaction (qRT-PCR)*

The levels of *Ifn-γ, GzmB, Prf* and *FasL* mRNAs were analyzed by qRT-PCR. Total RNA was isolated using TriZol reagent (Invitrogen), and cDNA was synthesized using the PrimeScript RT reagent kits (Takara) according to the manufacturers' instructions as previous reported[27]. The qRT-PCR was performed with SYBR Premix Ex Taq™ (Takara) and CFX96 Real-time system (Bio-Rad). The murine primer sequences used in PCR were as follows: *β-actin*, 5′-GAGACCTTCAACACCCCAGC and 3′-ATGTCACGCACGATTTCCC; *Ifn-γ*, 5′-ATGAACGCTACACACTGCATC and 3′-CATCCTTTTGCCAGTTCCTC; *Tnf-α*, 5′-AGTGACAAGCCTGTAGCCC and 3′-AGGTTGACTTTCTCCTGGTAT; *Prf*, 5′- AGCCCCTGCACACATTACTG and 3′-GCCCCTGCACACATTACTG; *FasL*, 5′-TCCGTGAGTTCACCAACCAAA and 3′-GGGGTTCCCTGTTAAATGGG. *GzmB*, 5′-CTGCTAAAGCTGAAGAGTAAGG and 3′-ACCTCTTTAGCGTGTTTGAG. The human primer sequences used in PCR were as follows: *β-actin*, 5′-GAGCTACGAGCTGCCTGACG and 3′-GTAGTTTCGTGGATGCCACAG; *Ifn-γ*, 5′-TGTTACTGCCAGGACCCATA and 3′-CTTCCTTGATGGTCTCCACA; *Prf*, 5′-TTCTCACAGTGGGAGCCAG and 3′-GGGCCACATGTAAAATCCAC; *GzmB*, 5′-AGGCTACCTAGCAACAAGGC and 3′-TCGATCTTCCTGCACTGTCA. The mRNA level was normalized to *β-actin*.

2.7. *Histology, immunohistochemistry (IHC) and immunofluorescence (IF)*

Tumor tissues were stained with H & E as per standard protocols, and analyzed by a pathologist under light microscope (Olympus). For all staining protocols, the sections were first deparaffinized, rehydrated and washed in 1% PBS–Tween. For IHC, the sections were treated with 2% hydrogen peroxide to block endogenous peroxidases, blocked with 3% goat serum, and incubated with specific primary antibodies for 2 h at room temperature. The sections were then incubated with streptavidin-HRP for 40 min, stained using DAB substrate and counter-stained with hematoxylin. For IF and TUNEL assay, the slides were stained with fluorescent labeled antibodies or TUNEL-FITC (1:100) respectively, and then counter-stained with DAPI for 5 min. Images were acquired by confocal laser-scanning microscope (Olympus FV1000). The integrated optical intensity of the respective markers in each sample was evaluated by Image-pro plus software.

2.8. *Intracellular staining*

The intracellular expression of cytokines in T-cells was analyzed using an eBioscience intracellular staining kit as previous reported[28]. Briefly, spleen cells from mice were incubated with PMA (100 ng/mL)/ionomycin (1 μg/mL) and monesine (1 μg/mL) in complete media at 37 °C for 6 h. The cells were first surface stained with CD4-FITC or CD8-APC for 15 min at 4 °C, then fixed and permeabilized with fixation and permeabilization wash buffers respectively. Cells were stained with PRF-PE, GZMB-FITC, TNF-α-FITC and IFN-γ-PE antibodies for 20 min, and then analyzed by flow cytometry analysis.

2.9. *Statistical analysis*

Data are presented as mean ± SEM, and compared using one-way ANOVA or Student's *t*-test as appropriate. Dunnett's test was used for comparing three or more groups. $P < 0.05$ was considered statistically significant.

3. Results

3.1. *SHP2 inhibition decreases tumor load in a xenograft tumor model*

To examine the effect of SHP2 inhibition on tumor maintenance, we established a subcutaneous xenograft tumor model in BALB/c mice using colon cancer CT-26 cells. On the 3rd day

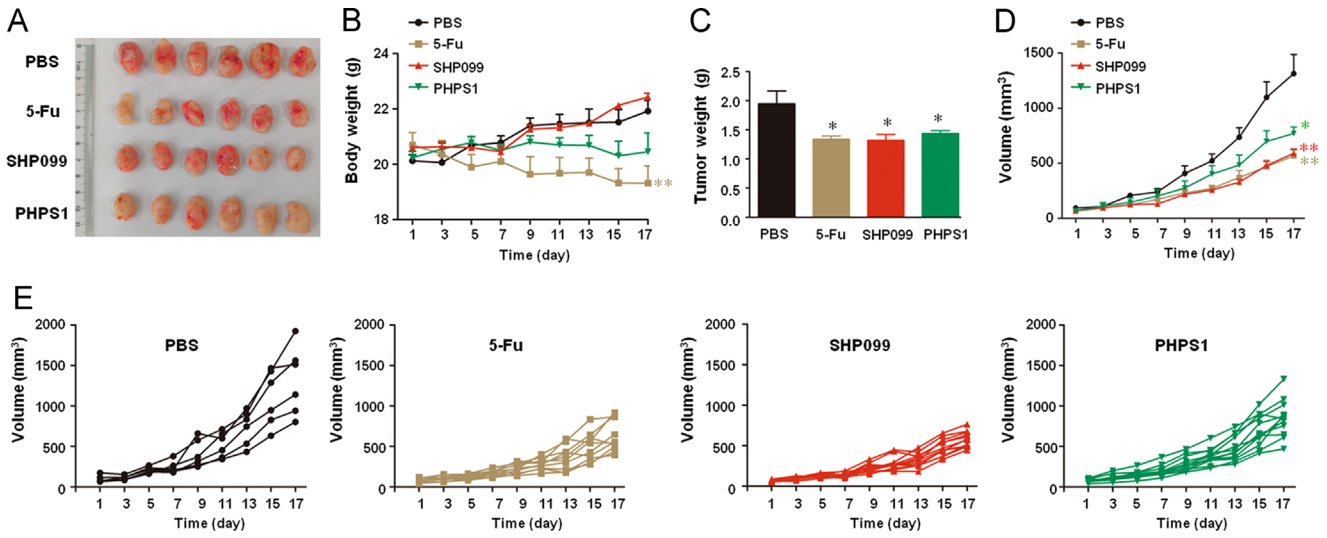

Figure 1 SHP2 inhibition decreases tumor load in CT-26 xenograft BALB/c mice. The mice were subcutaneously injected with 1×10^6 CT-26 colon cancer cells, and treated with 5-Fu (25 mg/kg i.p. every other day) and SHP099 or PHPS1 (5 mg/kg i.p. every day) from day 3 onwards. (A) Representative images. (B) Body weight of the mice. (C) Mean tumor weights of different groups. (D) Mean tumor volumes of different groups. (E) Tumor volumes of individual mice. Data are presented as mean ± SEM of 6 mice per group. $^{*}P < 0.05$, $^{**}P < 0.01$ *vs*. PBS.

post-inoculation, the mice were intraperitoneally injected with SHP2 inhibitor SHP099. Mice treated with 5-Fu were used as positive controls. Both tumor volume and weight were significantly decreased by SHP099 treatment (Fig. 1A–E), while no significant differences were seen in the body-weights of the SHP099-treated and vehicle treated mice. In contrast, 5-Fu remarkably reduced the body-weight of the mice (Fig. 1B), indicating a potent side-effect. The similar results were also obtained in another SHP2 inhibitor PHPS1 (Fig. 1A–E). Taken together, SHP2 inhibition suppressed tumor growth in CT-26 xenograft BALB/c mice without affecting the general health of the mice.

3.2. *SHP2 inhibition promotes cytokine/granule production by cytotoxic T-cells*

Histological analyses of H & E-stained tumor sections of the different groups (Fig. 2A) showed that SHP2 inhibition resulted in shrinkage, sparse arrangement and fragmentation of the tumor cells, indicating apoptosis of varying degrees. In addition, TUNEL staining confirmed that SHP2 inhibitors triggered extensive apoptosis in the tumor cells (Fig. 2B). To determine whether the anti-tumor immune response was enhanced by SHP2 inhibition, we detected the levels of cytokines/granules produced by cytotoxic T-cells in the tumors. The levels of IFN-γ and GZMB were markedly increased in tumor tissues treated with both SHP099 and PHPS1 (Fig. 2C). In addition, SHP2 inhibition also increased the levels of *Ifn-γ*, *Prf* and *GzmB* mRNA in tumors (Fig. 2D). Accordingly, SHP2 inhibition augmented the number of $CD8^+IFN\text{-}\gamma^+$ and $CD8^+GZMB^+$ cells in tumors (Fig. 2E and F). It should be noted that the number of $NK1.1^+IFN\text{-}\gamma^+$ cells was significantly increased upon the treatment of both SHP099 and PHPS1 (Supporting Information Fig. S1), suggesting that NK-mediated anti-tumor effect also contributes to SHP2 inhibition-triggered retardation of tumor growth. These data demonstrate that SHP2 inhibition increases the production of cytokines/granules by the cytotoxic T-cells.

3.3. *SHP2 inhibition does not retard tumor growth in nude mice*

To determine the underlying mechanism of SHP099-mediated anti-tumor effect, we analyzed the tumor dynamics in the nude mouse model. Interestingly, SHP099 did not decrease tumor volume and weight in the CT-26 xenograft BALB/c nude mice (Fig. 3A–E), and as shown by the TUNEL assay and PCNA expression (Fig. 3F–H), neither increased tumor cell apoptosis nor inhibited tumor growth. Furthermore, 0.3–10 μmol/L SHP099 did not inhibit the viability of the CT-26 cells in the MTT assay (Fig. 3I). These results indicate that SHP099 decreases tumor load through augmenting anti-tumor immunity rather than inhibiting growth of tumor cells in CT-26 colon cancer xenograft model.

3.4. *T cells-restricted ablation of SHP2 increases anti-tumor immune response*

To assess whether T-cells are responsible for the anti-tumor responses of SHP099, we used a T-cell specific SHP2 knockout ($Ptpn11^{Cd4-/-}$) mouse model. The mice were subcutaneously inoculated with 1×10^6 MC-38 colon cancer cells, and tumor size was measured from day 3 onwards. Compared to wild-type mice, $Ptpn11^{Cd4-/-}$ mice showed decreased tumor size and weight (Fig. 4A–D), and increased levels of *Ifn-γ*, *GzmB* and *Pfr* mRNA in the tumors (Fig. 4**E**). In addition, increased apoptosis (Fig. 4F and G) and cytokine/granule production was also seen in the tumor infiltrating $CD8^+$ T-cells (Fig. 4H and I) of $Ptpn11^{Cd4-/-}$ mice. These results suggest that SHP2 deficiency in T-cells augments anti-tumor immunity by enhancing the functions of $CD8^+$ cytotoxic T-cells.

3.5. *SHP2 inhibition synergizes with PD-1 blockade in tumor xenograft model*

Since SHP2 binds to several immune-inhibitory receptors including PD-1 and B- and T-lymphocyte attenuator (BTLA), we also tested for any synergistic effect between SHP2 inhibition and PD-1 blockade. To this end, we analyzed the *in vivo* efficacy of SHP099/anti-PD-1

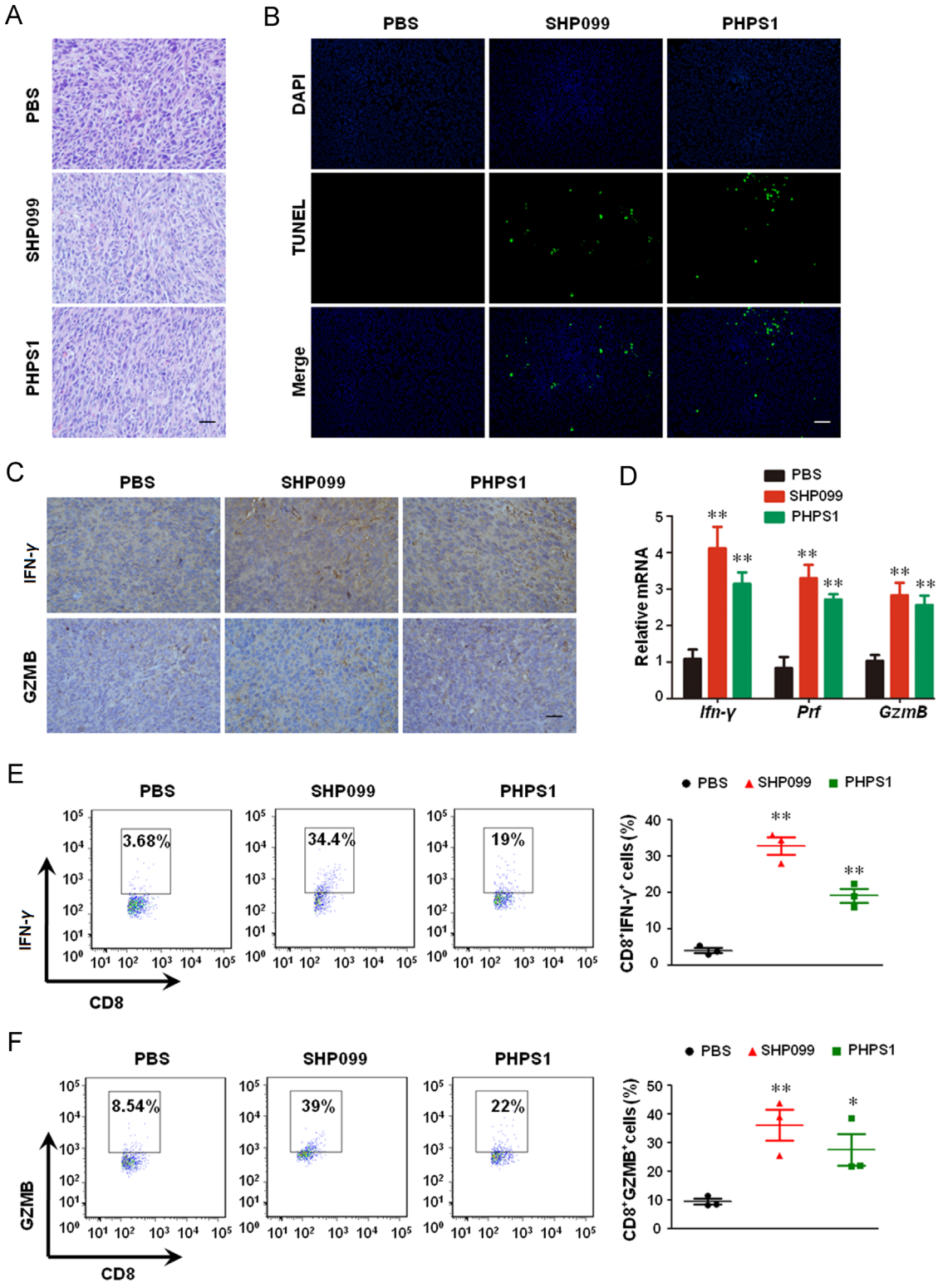

Figure 2 SHP2 inhibition promotes cytotoxic T-cell cytokine/granule production in CT-26 xenograft BALB/c mice. (A) H & E staining of tumor sections. (B) TUNEL assay for apoptotic cells in tumor tissue. (C) IHC for detecting IFN-γ and GZMB in the tumor sections. (D) qPCR for *Ifn-γ*, *Prf* and *GzmB* expression in tumors. Data are presented as mean ± SEM of 6 mice per group. (E) and (F) Intracellular staining for IFN-γ and GZMB production in tumor infiltrating $CD8^+$ T cells. Data are presented as mean ± SEM of 3 mice per group. $^*P < 0.05$, $^{**}P < 0.01$ *vs*. PBS. *Prf*, perforin; *GzmB*, granzyme B. Scale bar, 10 μm.

combination treatment in the murine syngeneic MC-38 colon cancer model. Mice treated with SHP099 and anti-PD-1 had significantly smaller tumors compared to mice receiving either SHP099 or anti-PD-1 monotherapy (Fig. 5A–E). Consequentially, combination of SHP099 and anti-PD-1 induced maximum apoptosis in the tumor cells (Fig. 5F and G), and also significantly increased the production of cytokines/

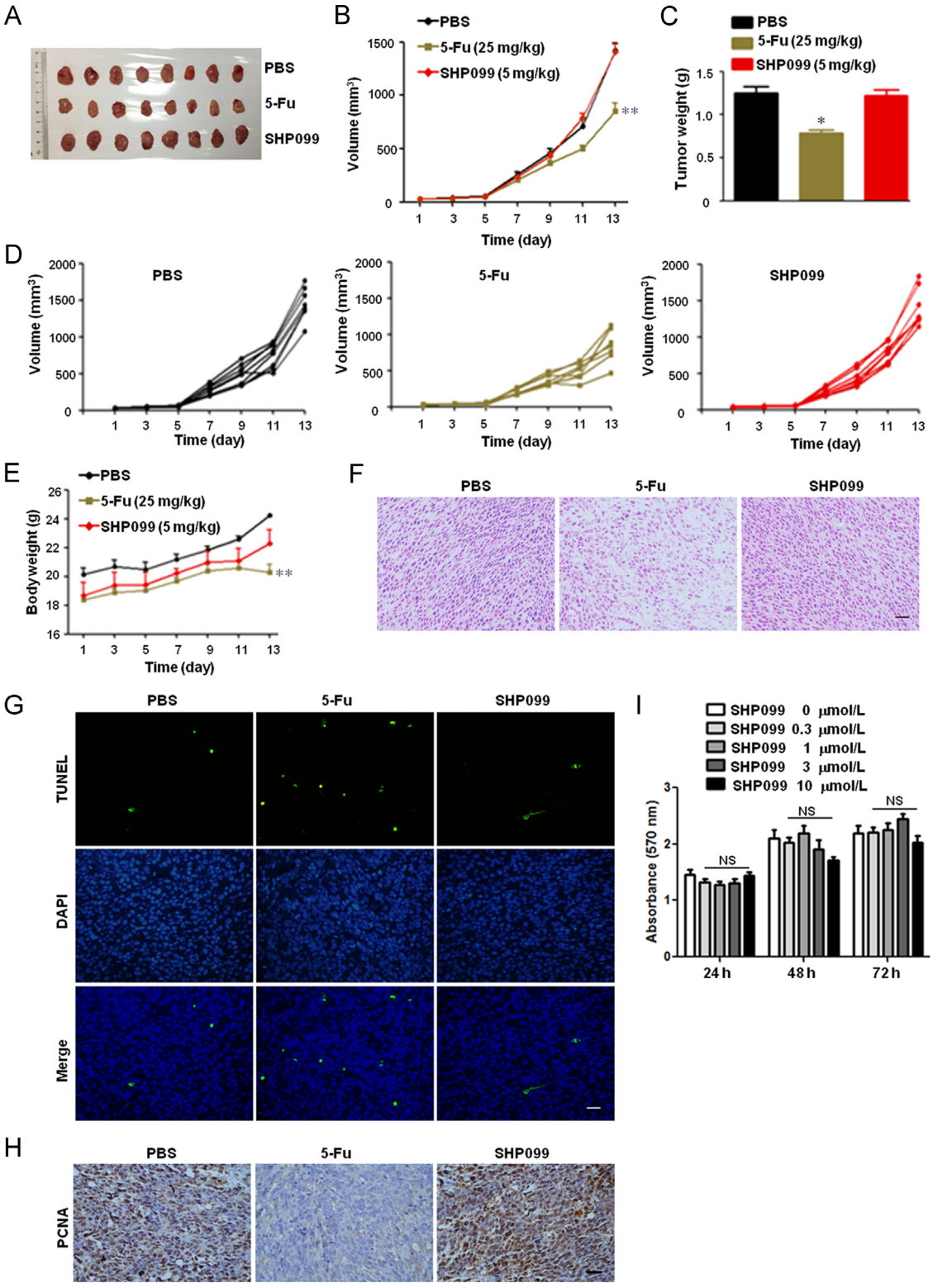

Figure 3 SHP2 inhibition has no effect on tumor size in CT-26 xenograft BALB/c nude mice. The mice were subcutaneously inoculated with 1×10^6 CT-26 colon cancer cells, and treated with 5-Fu (25 mg/kg i.p. every other day) and SHP099 (5 mg/kg i.p. every day) from day 3 onwards. (A) Representative images. (B) Mean tumor volumes of different groups. (C) Mean tumor weights of different groups. (D) Tumor volumes of individual mice. (E) Mean body weight of mice. Data in (B), (C), and (E) are presented as mean ± SEM of 8 mice per group. (F) H & E staining of tumor sections. (G) TUNEL assay for apoptotic cells in tumor tissue. (H) IHC for PCNA in tumor sections. (I) MTT viability assay for CT-26 colon cancer cells. Data are presented as mean ± SEM of three different experiments. $^{*}P < 0.05$, $^{**}P < 0.01$ *vs*. PBS. NS represents no significance *vs*. SHP099 (0 μmol/L). Scale bar, 10 μm.

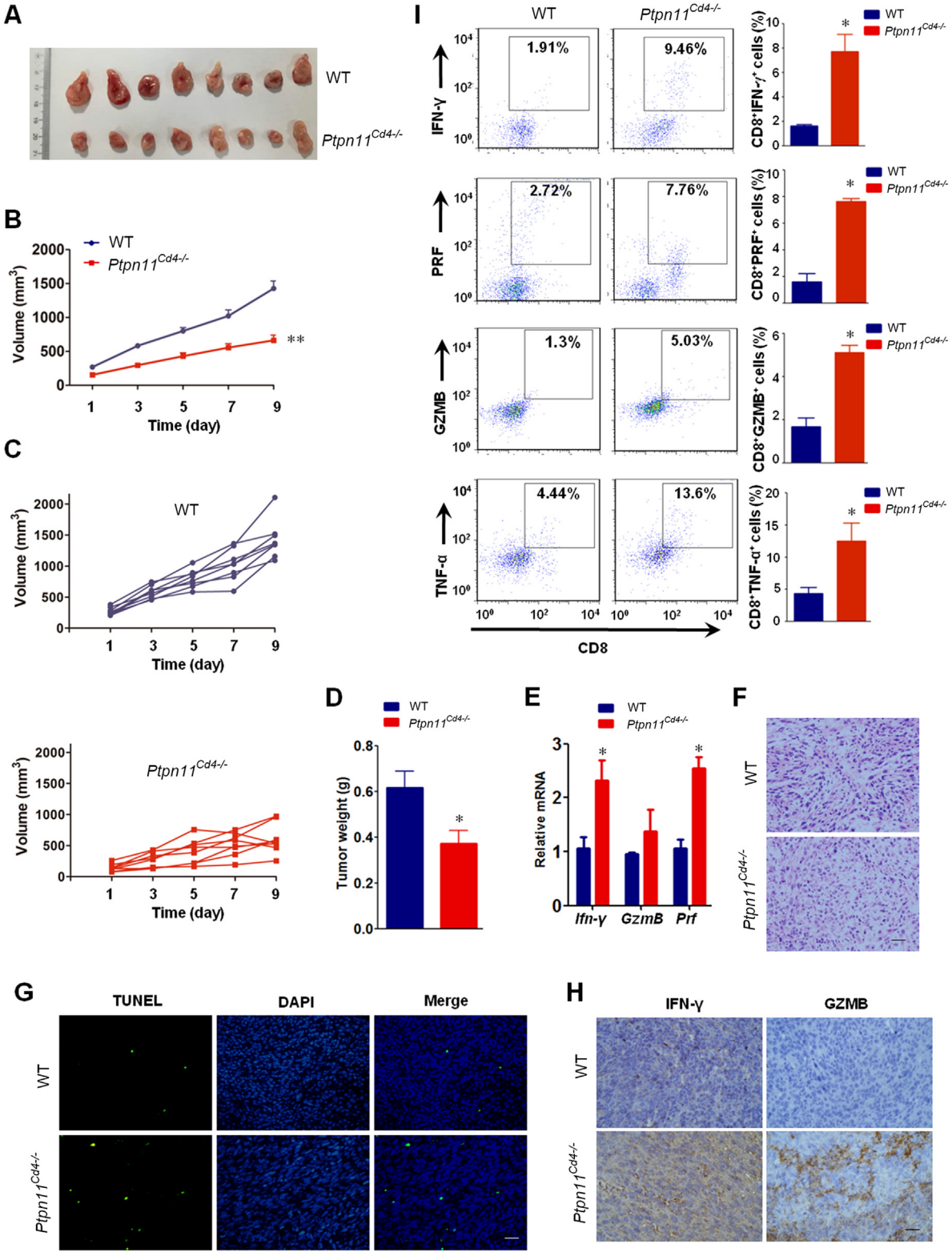

Figure 4 SHP2 deficiency in T-cells augments anti-tumor responses. T-cell specific SHP2 knockout mice ($Ptpn11^{Cd4-/-}$) were subcutaneously injected with 1×10^6 MC-38 colon cancer cells. (A) Representative images. (B) Mean tumor volumes of different groups. (C) Tumor volumes of individual mice. (D) Mean tumor weights of different groups. (E) qPCR assay for *Ifn-γ, GzmB* and *Prf* mRNA expression in the tumors. Data in (B), (D), and (E) are presented as mean ± SEM of 8 mice per group. (F) H & E staining of tumor sections. (G) TUNEL assay for apoptotic cells in tumor tissue. (H) IHC for IFN-γ and GZMB in tumor sections. (I) Intracellular staining for cytotoxic T-cell related cytokine/granule production in the tumor infiltrating $CD8^+$ T cells. Data are presented as mean ± SEM of 3 mice per group. $^*P < 0.05$, $^{**}P < 0.01$ *vs*. WT. *Prf*, perforin; *GzmB,* granzyme *B*. Scale bar, 10 μm.

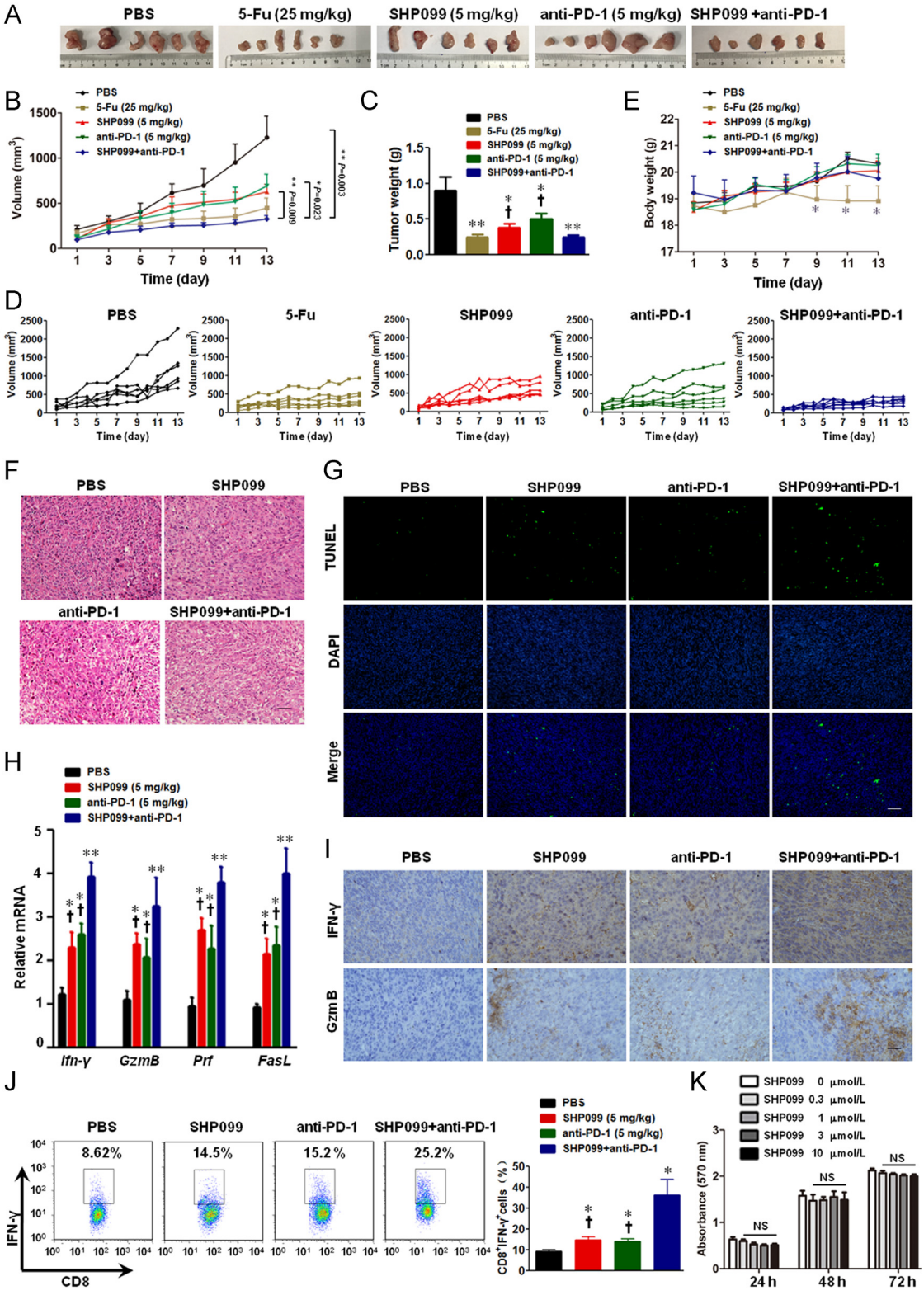

Figure 5 SHP2 inhibition synergizes with PD-1 blockade in MC-38 xenograft mice. The mice were subcutaneously inoculated with 1×10^6 MC-38 colon cancer cells, and treated with anti-PD-1 (5 mg/kg i.p. once every three days) and/or SHP099 (5 mg/kg i.p. every day) from day 3 onwards. All results presented are of day 13 post-inoculation. (A) Representative images of tumors. (B) Mean tumor volumes of different groups. (C) Mean tumor weights of different groups. (D) Tumor volume of individual mice. (E) Mean body weight of mice. (F) H & E staining of tumor sections. (G) TUNEL assay for apoptotic cells in tumor sections. (H) qPCR assay for the *Ifn-γ*, *GzmB*, *Prf* and *FasL* mRNA levels in tumor tissues. Data in (B), (C), (E), and (H) are presented as mean ± SEM of 6 mice per group. (I) IHC for IFN-γ and GZMB in tumor sections. (J) Intracellular staining for IFN-γ production in tumor infiltrating $CD8^+$ T cells. Data in (J) are presented as mean ± SEM of 3 mice per group. (K) MTT viability assay for MC-38 colon cancer cells. Data are presented as mean ± SEM of three different experiments. $^*P < 0.05$, $^{**}P < 0.01$ *vs*. PBS. $^\dagger P < 0.05$ *vs*. SHP099+anti-PD-1. *Prf*, perforin; *GzmB*, granzyme B. Scale bar, 10 μm.

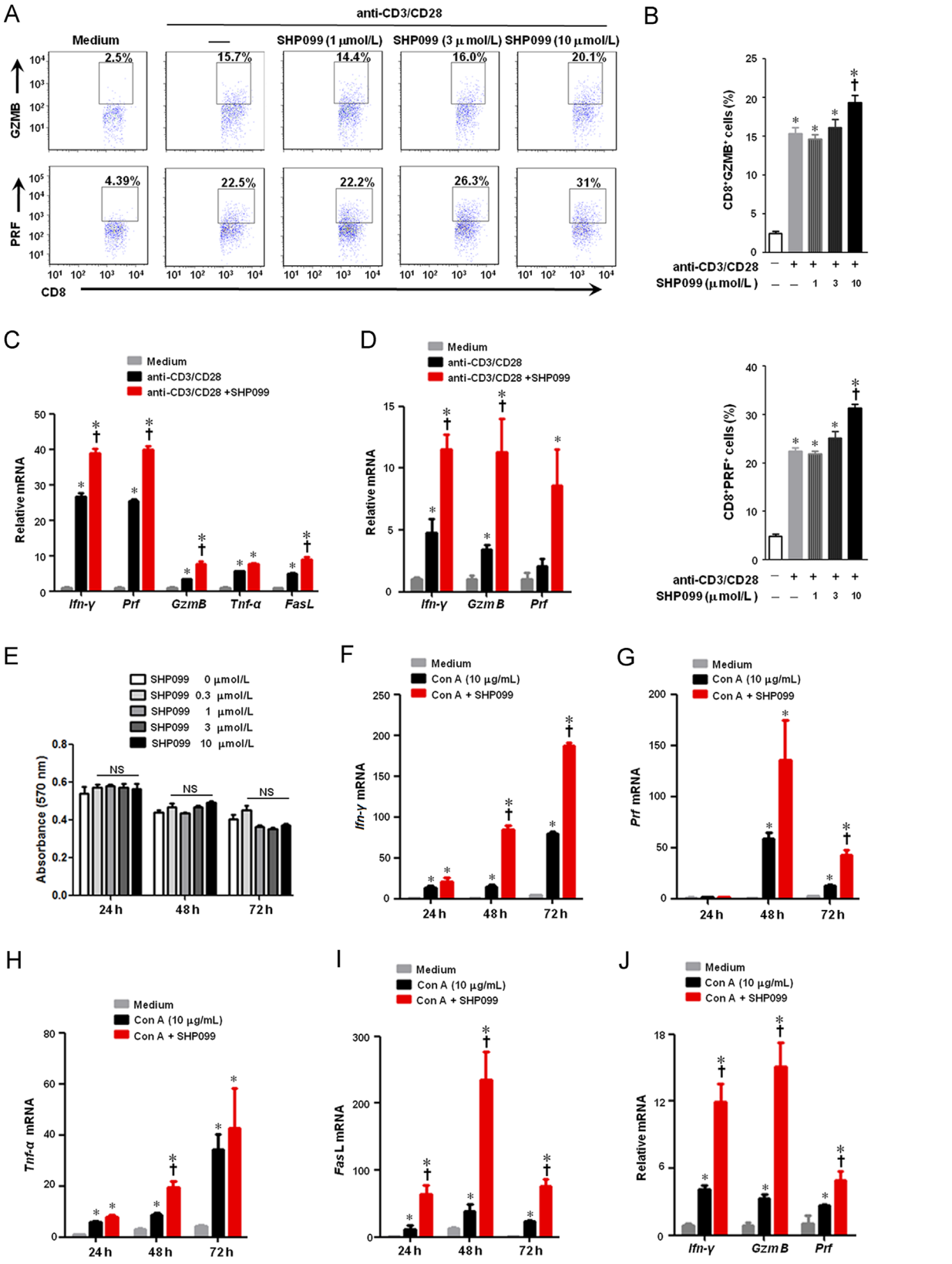

Figure 6 SHP2 inhibition enhances the activation of $CD8^+$ cytotoxic T lymphocytes *in vitro*. (A)–(C) Murine splenic $CD8^+$ T cells were incubated with various concentrations of SHP099 for 24 h in the presence of plate-bound 0.5 μg/mL murine anti-CD3 and 0.5 μg/mL murine anti-CD28. (A) and (B) Flow cytomytry assay for detecting GZMB and PRF in $CD8^+$ T cells. (C) qPCR assay for mRNA expressions of *Ifn-γ, Prf, GzmB, FasL* and *Tnf-α* in $CD8^+$ T cells. (D) Human peripheral blood mononuclear cells (PBMCs) were incubated with 10 μmol/L SHP099 for 24 h in the presence of plate-bound 0.25 μg/mL human anti-CD3 and 1 μg/mL human anti-CD28. Relative mRNA levels of *Ifn-γ, GzmB* and *Prf* were measured by qPCR assay. (E) MTT assay for murine splenic $CD8^+$ T cell viability. (F)–(I) Murine splenic cells were incubated with 10 μmol/L SHP099 for 24 h in the presence of 10 μg/mL Con A. Relative mRNA expressions of *Ifn-γ, Prf, Tnf-α* and *FasL* were measured by qPCR assay. (J) Human PBMCs were incubated with 10 μmol/L SHP099 for 24 h in the presence of 10 μg/mL Con A. Relative mRNA levels of *Ifn-γ, GzmB* and *Prf* were measured by qPCR assay. Data are presented as mean ± SEM of three different experiments. $^*P < 0.05$ *vs.* Medium. $^\dagger P < 0.05$ *vs.* anti-CD3/CD28 or Con A. NS represents no significance. *Prf*, perforin; *GzmB*, granzyme B.

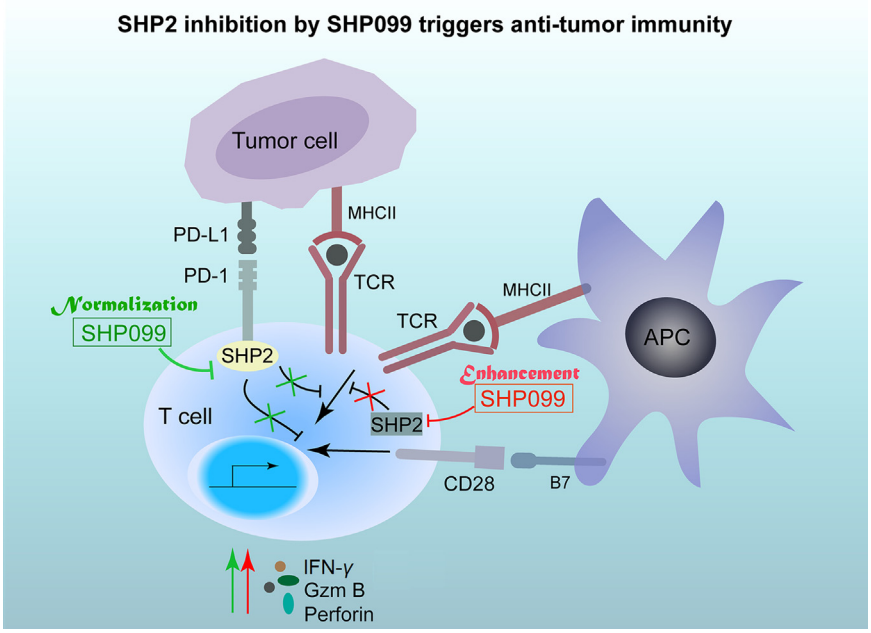

Figure 7 The graphic illustration of the mechanism of SHP2 inhibition by SHP099 in triggering anti-tumor immunity. On one hand, SHP2 inhibition by its allosteric inhibitor SHP099 reverses the inhibitory effect on T cells triggered by PD-L1-expressing cancer cells, which is called "normalization" of anti-tumor immunity (Green). On the other hand, SHP2 inhibition also contributes to T cell activation, which is called "enhancement" of anti-tumor immunity (Red). Both "normalization" and "enhancement" of anti-tumor immunity by SHP2 inhibition are responsible for anti-tumor effect of SHP099 *in vivo*.

granules by the cytotoxic T-cells (Fig. 5H and I). Furthermore, IFN-γ production in the tumor infiltrating CD8$^+$ T-cells was most significantly upregulated in the combination-therapy group (Fig. 5J). However, the number of splenic Treg cells were comparable across the treatment groups (Supporting Information Fig. S2), suggesting that Tregs are dispensable for the anti-tumor effect of SHP099. Similar synergistic anti-tumor effects were seen in the colorectal carcinoma CT-26 xenograft model as well (Supporting Information Fig. S3). It should be noted that SHP099 in a range from 0.3–10 μmol/L did not inhibit the viability of colon cancer MC-38 cells by MTT assay (Fig. 5K). Taken together, inhibition of both SHP2 and PD-1 checkpoint synergistically activated T-cells in the tumor xenograft model, and retarded tumor growth.

3.6. *SHP2 inhibition enhances the activation of CD8$^+$ cytotoxic T lymphocytes in vitro*

Although SHP2 inhibition augmented CD8$^+$ T cell activation *in vivo*, it was not clear whether SHP099 directly affected T cells. Splenic T-cells were treated with SHP099 in the presence of anti-CD3 and anti-CD28 for 24 h. SHP2 inhibition by SHP099 augmented production of both GZMB and PRF in the CD8$^+$ T-cells in a dose-dependent manner, with maximal effects at 10 μmol/L (Fig. 6A and B). In addition, SHP099 also up-regulated the *Ifn-γ, GzmB* and *Prf* mRNA levels in both murine CD8$^+$ T-cells (Fig. 6C) and human PBMCs (Fig. 6D), but did not affect the viability of CD8$^+$ T-cells (Fig. 6E). Moreover, SHP099 significantly enhanced the mRNA levels of cytotoxic T-cell-related cytokine/granule in murine splenic cells (Fig. 6F–I) or human PBMCs (Fig. 6J) stimulated by mitogen Con A. Taken together, these results suggest that SHP2 inhibition with SHP099 enhances the activation and function of CD8$^+$ cytotoxic T-cells *in vitro*.

4. Discussion

SHP2 has recently attracted a lot of attention in cancer immunotherapy. While it shows an oncogenic role in a number of cancer types including leukemia, liver cancer, and breast cancers[13,15,29], it can also regulate T-cell exhaustion by interacting with various inhibitory immune checkpoint receptors such as PD-1 and BTLA[25,30]. SHP2 binds with PD-1 following PD-L1 stimulation and inhibits T cell activation, which makes it a promising target for cancer immunotherapy. Therefore, SHP2 inhibitors have been considered for cancer therapy as per the "one stone two birds" approach of inhibiting tumor cell proliferation and activating T-cell anti-tumor immunity. In the present study, we demonstrated that a unique SHP2 allosteric inhibitor SHP099 inhibited tumor growth and synergized with anti-PD-1 antibody by augmenting CD8$^+$ T-cell dependent anti-tumor immunity.

In contrast to the SHP2 inhibitors that bind to the catalytic domain of SHP2, SHP099 is a unique allosteric inhibitor[16,31] that acts as a "molecule glue" which selectively blocks SHP2 activity by locking it in an auto-inhibited conformation. Although the *in vitro* and *in vivo* anti-tumor effects of SHP099 have been well documented[16,31], the underlying mechanisms were still unclear. To address this, we used a CT-26 colon cancer xenograft model since CT-26 cells are insensitive to SHP099 (Fig. 3). Interestingly, while SHP099 barely inhibited CT-26 tumor growth in the immunodeficient nude mice (Fig. 3), it significantly decreased the tumor load in CT-26 engrafted mice with an intact immune system (Fig. 1). SHP099 treatment significantly elevated the proportion of CD8$^+$IFN-γ^+ and CD8$^+$GZMB$^+$ T-cells, as well as the expression of cytotoxicity-related genes including *GzmB* and *Prf* (Fig. 2). These results suggest that SHP099 retarded tumor growth by boosting anti-tumor immunity in the mice.

SHP2 inhibition is known to promote T-cell activation, and several reports including our own previous study have shown that SHP2 conditional knockout has no major effects on T-cell development, while T-cell activation or differentiation may be affected under pathological circumstances[26,32]. Overexpression of a catalytically inactive form of SHP2 carrying a classic cysteine 459-to-serine mutation reduced T-cell activation[33]. Furthermore, a small-molecule compound named fusaruside triggered phosphorylation of SHP2 resulting in a reduction in Th1 cytokine production[34]. In our study, treatment with SHP099 increased IFN-γ and GZMB production by $CD8^+$ T-cells suggesting that SHP2 inhibition can also boost $CD8^+$ T-cell activation and contribute to anti-tumor immunity.

SHP2 inhibition also relieves the inhibitory effect on T-cells triggered by PD-L1-expressing cancer cells. Two mechanisms have been proposed for PD-L1 induced inhibition of T-cells. Following PD-L1 stimulation, PD-1 clusters with TCR and SHP2, which induces the de-phosphorylation of the proximal TCRs and suppresses T-cell activation[25]. Another study demonstrated that PD-1/PD-L1 suppressed T-cell function primarily by inactivating CD28 signaling[23]. Consistent with this, the combination of SHP099 and anti-PD-1 antibody significantly increased the tumor inhibitory effect as both nodes of PD-1 signaling were blocked. We hypothesize therefore that this combination may increase the response of patients to the immune checkpoint inhibitors. In addition, the RTK-dependent tumors have been shown to be sensitive to SHP2 inhibitors[16]. Taken together, fostering anti-tumor immunity by blocking PD-1 and PD-L1 along with SHP2 would be more effective.

Based on the above findings, it is reasonable to surmise that SHP2 inhibition would augment anti-tumor immunity and retard *in vivo* tumor growth. Recently, Rota et al.[35] showed that SHP2 was dispensable for T-cell depletion and PD-1 signaling *in vivo*, based on the observation that mice with SHP2-deficient T-cells responded similarly as the controls to anti-PD-1 treatment. Although anti-PD-1 antibody was still beneficial in mice with SHP2-deficient T-cells, one could not rule out the possibility that SHP2 also played an important role in PD-1-mediated T-cell exhaustion. Another possibility is that T-cell is not the only target of anti-PD-1 antibody. Kleffel et al.[36] demonstrated that murine and human melanomas contained PD-1-expressing subpopulations which promoted tumorigenesis, suggesting that targeting the endogenous PD-1 in cancer cells would significantly augment the therapeutic efficacy of anti-PD-1 antibody. Notably, Rota et al.[35] did not observe any significant improvement in the tumor size of mice with SHP2-deficient T-cells, although the growth of tumors in these mice was markedly slower compared to the wide type mice. On day 22 post-tumor cell inoculation, all tumors (10/10) in the $Shp2^{flox/flox}$ group reached 1000 mm^3, while only 5/9 tumors in the *Cd4*-Cre:$Shp2^{flox/flox}$ group reached that size. In addition, all $Shp2^{flox/flox}$ mice died by day 23 while the *Cd4*-Cre:$Shp2^{flox/flox}$ mice survived till day 32. This clearly suggested that SHP2-deficiency in T-cells decreased the tumor load and improved survival. In agreement with the above, we found that T cell-restricted ablation of SHP2 inhibited tumor growth by augmenting anti-tumor responses (Fig. 4).

In summary, our study shows that the SHP2 allosteric inhibitor SHP099 is a promising drug candidate for cancer immunotherapy. SHP2 inhibition both enhances and normalizes anti-tumor immunity, and the combination of SHP099 and anti-PD-1 is a potentially robust therapeutic strategy for cancer control (Fig. 7).

Acknowledgments

We thank Dr. Chong Sun (The Netherlands Cancer Institute, The Netherlands) for valuable advice on this project. This work was supported by National Natural Science Foundation of China (Nos. 81673436, 21472091, 81872877, 81673437), Mountain-Climbing Talents Project of Nanjing University, the Open Fund of State Key Laboratory of Pharmaceutical Biotechnology, Nanjing University (No. KF-GN-201703, China), Open Project Program of Jiangsu Key Laboratory for Pharmacology and Safety Evaluation of Chinese Materia Medica (No. JKLPSE201802, China) and the Project of the Priority Academic Program Development of Jiangsu Higher Education Institutions (PAPD, China).

Appendix A. Supporting information

Supplementary data associated with this article can be found in the online version at https://doi.org/10.1016/j.apsb.2018.08.009.

References

1. Chen L, Flies DB. Molecular mechanisms of T cell co-stimulation and co-inhibition. *Nat Rev Immunol* 2013;**13**:227–42.
2. Parry RV, Chemnitz JM, Frauwirth KA, Lanfranco AR, Braunstein I, Kobayashi SV, et al. CTLA-4 and PD-1 receptors inhibit T-cell activation by distinct mechanisms. *Mol Cell Biol* 2005;**25**:9543–53.
3. Munn DH, Bronte V. Immune suppressive mechanisms in the tumor microenvironment. *Curr Opin Immunol* 2016;**39**:1–6.
4. Ostrand-Rosenberg S, Horn LA, Haile ST. The programmed death-1 immune-suppressive pathway: barrier to antitumor immunity. *J Immunol* 2014;**193**:3835–41.
5. Pardoll DM. The blockade of immune checkpoints in cancer immunotherapy. *Nat Rev Cancer* 2012;**12**:252–64.
6. Lines JL, Pantazi E, Mak J, Sempere LF, Wang L, O'Connell S, et al. VISTA is an immune checkpoint molecule for human T cells. *Cancer Res* 2014;**74**:1924–32.
7. Kane LP. T cell Ig and mucin domain proteins and immunity. *J Immunol* 2010;**184**:2743–9.
8. Andrews LP, Marciscano AE, Drake CG, Vignali DA. LAG3 (CD223) as a cancer immunotherapy target. *Immunol Rev* 2017;**276**:80–96.
9. Feng GS, Hui CC, Pawson T. SH2-containing phosphotyrosine phosphatase as a target of protein-tyrosine kinases. *Science* 1993;**259**:1607–11.
10. Hof P, Pluskey S, Dhe-Paganon S, Eck MJ, Shoelson SE. Crystal structure of the tyrosine phosphatase SHP-2. *Cell* 1998;**92**:441–50.
11. Qu CK. The SHP-2 tyrosine phosphatase: signaling mechanisms and biological functions. *Cell Res* 2000;**10**:279–88.
12. Liu JJ, Li Y, Chen WS, Liang Y, Wang G, Zong M, et al. SHP2 deletion in hepatocytes suppresses hepatocarcinogenesis driven by oncogenic β-catenin, PIK3CA and MET. *J Hepatol* 2018;**69**:79–88.
13. Aceto N, Sausgruber N, Brinkhaus H, Gaidatzis D, Martiny-Baron G, Mazzarol G, et al. Tyrosine phosphatase SHP2 promotes breast cancer progression and maintains tumor-initiating cells *via* activation of key transcription factors and a positive feedback signaling loop. *Nat Med* 2012;**18**:529–37.
14. Liu KW, Feng HZ, Bachoo R, Kazlauskas A, Smith EM, Symes K, et al. SHP-2/PTPN11 mediates gliomagenesis driven by PDGFRA and INK4A/ARF aberrations in mice and humans. *J Clin Invest* 2011;**121**:905–17.
15. Xu RZ, Yu Y, Zheng S, Zhao XY, Dong QH, He ZW, et al. Overexpression of SHP2 tyrosine phosphatase is implicated in leukemogenesis in adult human leukemia. *Blood* 2005;**106**:3142–9.

16. Chen YN, LaMarche MJ, Chan HM, Fekkes P, Garcia-Fortanet J, Acker MG, et al. Allosteric inhibition of SHP2 phosphatase inhibits cancers driven by receptor tyrosine kinases. *Nature* 2016;**535**:148–52.
17. Matozaki T, Murata Y, Saito Y, Okazawa H, Ohnishi H. Protein tyrosine phosphatase SHP-2: a proto-oncogene product that promotes Ras activation. *Cancer Sci* 2009;**100**:1786–93.
18. Mainardi S, Mulero-Sanchez A, Prahallad A, Germano G, Bosma A, Krimpenfort P, et al. SHP2 is required for growth of KRAS-mutant non-small-cell lung cancer *in vivo*. *Nat Med* 2018;**24**:961–7.
19. Ruess DA, Heynen GJ, Ciecielski KJ, Ai J, Berninger A, Kabacaoglu D, et al. Mutant KRAS-driven cancers depend on PTPN11/SHP2 phosphatase. *Nat Med* 2018;**24**:954–60.
20. Wong GS, Zhou J, Liu JB, Wu Z, Xu X, Li T, et al. Targeting wild-type KRAS-amplified gastroesophageal cancer through combined MEK and SHP2 inhibition. *Nat Med* 2018;**24**:968–77.
21. Tajan M, de Rocca Serra A, Valet P, Edouard T, Yart A. SHP2 sails from physiology to pathology. *Eur J Med Genet* 2015;**58**:509–25.
22. Salmond RJ, Alexander DR. SHP2 forecast for the immune system: fog gradually clearing. *Trends Immunol* 2006;**27**:154–60.
23. Hui E, Cheung J, Zhu J, Su X, Taylor M, Wallweber H, et al. T cell costimulatory receptor CD28 is a primary target for PD-1-mediated inhibition. *Science* 2017;**355**:1428–33.
24. Li J, Jie HB, Lei Y, Gildener-Leapman N, Trivedi S, Green T, et al. PD-1/SHP-2 inhibits Tc1/Th1 phenotypic responses and the activation of T cells in the tumor microenvironment. *Cancer Res* 2015;**75**:508–18.
25. Yokosuka T, Takamatsu M, Kobayashi-Imanishi W, Hashimoto-Tane A, Azuma M, Saito T. Programmed cell death 1 forms negative costimulatory microclusters that directly inhibit T cell receptor signaling by recruiting phosphatase SHP2. *J Exp Med* 2012;**209**:1201–17.
26. Liu W, Guo W, Shen L, Chen Z, Luo Q, Luo X, et al. T lymphocyte SHP2-deficiency triggers anti-tumor immunity to inhibit colitis-associated cancer in mice. *Oncotarget* 2017;**8**:7586–97.
27. Peng S, Hang N, Liu W, Guo W, Jiang C, Yang X, et al. Andrographolide sulfonate ameliorates lipopolysaccharide-induced acute lung injury in mice by down-regulating MAPK and NF-kappaB pathways. *Acta Pharm Sin B* 2016;**6**:205–11.
28. Sang X, Wang R, Han Y, Zhang C, Shen H, Yang Z, et al. T cell–associated immunoregulation and antiviral effect of oxymatrine in hydrodynamic injection HBV mouse model. *Acta Pharm Sin B* 2017;**7**:311–8.
29. Han T, Xiang DM, Sun W, Liu N, Sun HL, Wen W, et al. PTPN11/Shp2 overexpression enhances liver cancer progression and predicts poor prognosis of patients. *J Hepatol* 2015;**63**:650–60.
30. Sedy JR, Gavrieli M, Potter KG, Hurchla MA, Lindsley RC, Hildner K, et al. B and T lymphocyte attenuator regulates T cell activation through interaction with herpesvirus entry mediator. *Nat Immunol* 2005;**6**:90–8.
31. Garcia Fortanet J, Chen CH, Chen YN, Chen Z, Deng Z, Firestone B, et al. Allosteric inhibition of SHP2: identification of a potent, selective, and orally efficacious phosphatase inhibitor. *J Med Chem* 2016;**59**:7773–82.
32. Miah SM, Jayasuriya CT, Salter AI, Reilly EC, Fugere C, Yang W, et al. *Ptpn11* deletion in $CD4^{+}$ cells does not affect T cell development and functions but causes cartilage tumors in a T cell-independent manner. *Front Immunol* 2017;**8**:1326.
33. Dong B, Gao Y, Zheng X, Gao G, Gu H, Chen X, et al. T cell activation is reduced by the catalytically inactive form of protein tyrosine phosphatase SHP-2. *Int J Clin Exp Med* 2015;**8**:6568–77.
34. Wu X, Guo W, Wu L, Gu Y, Gu L, Xu S, et al. Selective sequestration of STAT1 in the cytoplasm *via* phosphorylated SHP-2 ameliorates murine experimental colitis. *J Immunol* 2012;**189**:3497–507.
35. Rota G, Niogret C, Dang AT, Barros CR, Fonta NP, Alfei F, et al. Shp-2 is dispensable for establishing T cell exhaustion and for PD-1 signaling *in vivo*. *Cell Rep* 2018;**23**:39–49.
36. Kleffel S, Posch C, Barthel SR, Mueller H, Schlapbach C, Guenova E, et al. Melanoma cell-intrinsic PD-1 receptor functions promote tumor growth. *Cell* 2015;**162**:1242–56.